Submitted to

14th International Workshop on Deep Inelastic Scattering, DIS2006, April 20-24, 2006, Tsukuba, Japan

www-h1.desy.de/h1/www/publications/conf/conf_list.html

H1prelim-06-032

Azimuthal Correlations in Dijet Events from Deep Inelastic Electron-Proton Scattering at HERA

H1 Collaboration

Abstract

Correlations in the azimuthal angle between dijets produced in deep inelastic e^+p scattering events, collected by the H1 experiment during 1999-2000, have been investigated. Cross sections are presented as a function of the azimuthal separation between the two jets in the hadronic center of mass frame, $\Delta\phi^*$, in different regions of the photon virtuality Q^2 and in different regions of the Bjorken scaling variable x_{Bj}. The results are compared to the predictions of QCD Monte Carlo Models as well as to NLO di-jet (α_s^2) and NLO three-jet (α_s^3) calculations.

1 Introduction

In deep inelastic ep-collisions, dijets are in leading order (LO) produced via the boson-gluon fusion (BGF) and QCD-Compton (QCD-C) processes, where the former dominates at small x. In the DGLAP approximation [1], the gluon is in leading order assumed to be collinear with the proton direction. Thus, the two jets produced will be back-to-back in the hadronic center of mass (HCM) frame since the photon and the gluon collide head-on. The azimuthal angle between the two jets will in this scenario be[1] $\Delta\phi^* \approx \pi$ and configurations with $\Delta\phi^* < \pi$ can only originate from higher order initial or final state radiation. Initial state radiation is in the DGLAP approximation ordered in k_t such that the acquired transverse momentum of the interacting gluon is restricted.

However, at small x the evolution of the gluon ladder may follow a different dynamic with emissions unordered in k_t such that the gluon interacting with the photon may take any kinematically allowed transverse momentum. This would give a broader $\Delta\phi^*$ spectrum [2] compared to DGLAP. Also, in approximations using unintegrated gluon densities, e.g. BFKL [3] and CCFM [4], the gluon has an initial transverse momentum already in LO. Hence, azimuthal correlations could be used to distinguish between DGLAP and other dynamics at small x and also to constrain the unintegrated gluon density.

2 Event Selection

In this analysis, positron-proton data collected by the H1 experiment during 1999-2000 is used, corresponding to an integrated luminosity of $\mathcal{L}_{int} = 64.3$ pb^{-1}. Deep inelastic scattering (DIS) events are selected by requiring a highly energetic electron in the SPACAL calorimeter,

$$\begin{aligned} E_e^{'} &> 9 \text{ GeV} \\ 156^\circ < \theta_e &< 175^\circ \end{aligned}$$

where $E_e^{'}$ and θ_e is the energy and polar angle of the scattered electron, respectively. The photon virtuality, Q^2, and the inelasticity, y, are determined using the electron method [7] and must fulfill

$$\begin{aligned} 5 \text{ GeV}^2 < Q^2 &< 100 \text{ GeV}^2 \\ 0.1 < y &< 0.7 \end{aligned}$$

The jet selection was performed using the inclusive k_t-algorithm [8] applied to objects combining tracks and calorimetric clusters [9] in the HCM frame. To ensure a good jet reconstruction it is required that

$$\begin{aligned} -1 < \eta_j &< 2.5 \\ E_{T,j}^* &> 5 \text{ GeV}. \end{aligned}$$

Here, the pseudo-rapidity $\eta_j = -\ln(\tan(\theta_j/2))$ where θ_j is the polar angle of the jet, and $E_{T,j}^*$ is the transverse energy of the jet in the HCM frame. If more than two jets fulfill these criteria, the two jets closest to the scattered electron in η are chosen as the dijet system.

[1]Observables in the HCM frame are labeled with a *.

3 Correction Procedure and Systematic Uncertainties

Data is corrected for limited detector resolution and acceptance using a bin-by-bin procedure. Correction factors are determined using detector simulated events, where QED radiation has been taken into account, generated by the Monte Carlo (MC) programs DJANGO(CDM) and RAPGAP(DIR). The average correction factor obtained from the two MC generators are applied to the data.

The following systematic uncertainties are considered and added in quadrature with the statistical uncertainty of the data:

- The positron energy has been varied by $\pm$ 1%
- The positron polar angle has been varied by $\pm$1 mrad
- The LAr hadronic energy has been varied by $\pm$ 4%
- The track momentum has been varied by $\pm$ 3%
- The model dependence is estimated as half of the difference between the correction factors obtained by the two MC generators
- Photoproduction background is estimated using detector simulated MC events from the PHOJET [10] generator. For the dijet samples, this background is negligible
- The luminosity is determined to a precision of $\pm$ 1.5%, which is taken as an overall systematic uncertainty

4 QCD Models and NLO Calculations

The experimental data are compared to the predictions of several MC generators as well as NLO calculations. RAPGAP [11] uses LO matrix elements (ME) and evolves the parton ladder according to the LL DGLAP equation. QED radiation is included using HERACLES [12]. In addition, RAPGAP offers the possibility to use resolved photons. The parton density functions (PDFs) CTEQ6L [13] and SaS-G 1D [14] are used for the proton and the photon, respectively.

The program CASCADE [15] uses the CCFM equation for the evolution of the parton ladder. Cross sections are obtained by convoluting LO off-shell ME with unintegrated parton density functions (uPDFs). Here, the uPDFs A0 [16] and J2003(set2) [17] was used.

The DJANGOH [18] program provides an interface between HERACLES and LEPTO [19]. LEPTO, which is based on LO matrix elements and DGLAP parton showers, can be used together with ARIADNE [20], simulating parton showers according to the color dipole model (CDM).

All the generators above use the Lund string model [21] as implemented in JETSET [22] for the hadronisation process.

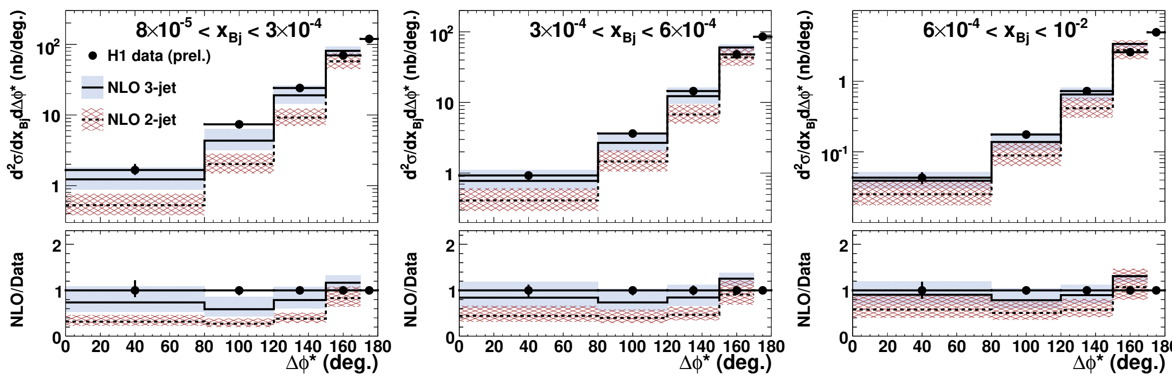

Figure 1: *Dijet cross sections as a function of $\Delta\phi^*$ in bins of x_{Bj}. Data are compared to NLO 3-jet (full line) and NLO 2-jet (dashed line) calculations obtained using the NLOJET++ program. The error band represent the scale uncertainty as described in the text.*

NLO di-jet (α_s^2) and NLO three-jet (α_s^3) calculations are obtained using the NLOJET++ [23] program. The renormalisation scale μ_r and factorisation scale μ_f are chosen as the average transverse energy of the two jets, $\mu_r = \mu_f = \left(\frac{E^*_{T1}+E^*_{T2}}{2}\right)$. Corrections for hadronisation effects are made bin-by-bin using CASCADE with the KMR [24] and A0 uPDFs for the di-jet and three-jet case, respectively. For the NLO calculations, the PDF CTEQ6M [13] is used. The scale uncertainties are estimated by varying μ_r and μ_f simultaneously a factor 2 up and 1/2 down.

5 Results

In Figure 1 is shown the dijet cross section as a function of the azimuthal angle $\Delta\phi^*$ in bins of x_{Bj} compared to NLO 2-jet and NLO 3-jet calculations. Below the cross sections are also shown the ratio of the theoretical predictions and measured data. Statistical uncertainties are shown as inner error bars, while the outer error bars show the total uncertainty (statistic and systematic uncertainties added in quadrature). Beacause of infrared sensitivity, the NLO calculations give no predictions in the back-to-back bins ($170° < \Delta\phi^* < 180°$). The NLO 2-jet calculation, which effectively is a LO prediction for this observable, is clearly not sufficient to describe the data. The NLO 3-jet calculation, effectively being an NLO prediction, is closer to the data but is systematically low for $\Delta\phi^* < 150°$. However, the scale uncertainties are large, typically 20 - 50%, and cover the data in most bins. When normalising the data to the visible cross section between $0° < \Delta\phi^* < 170°$ in each x_{Bj} bin, there is cancellation of the scale uncertainties for the NLO calculations, shown in Figure 2. As can be seen, the data is no longer within the scale uncertainties of the NLO 3-jet calculation.

Figure 3 shows the same data as in Figure 1 compared to the predictions of CASCADE using two different uPDFs. Whereas CASCADE (J2003) describes the data fairly well in all but the lowest x_{Bj} bin, CASCADE (A0) fails to describe the data in all bins, predicting too many jets with small $\Delta\phi^*$. This indicates that the k_t-spectrum of the A0 uPDF is too hard.

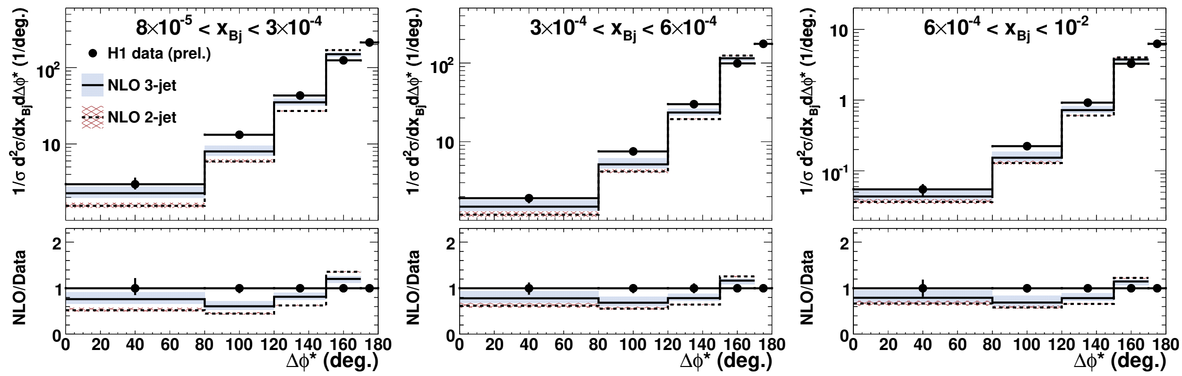

Figure 2: *Dijet cross sections as a function of $\Delta\phi^*$ in bins of x_{Bj} and normalised to the visible cross section between $0^\circ < \Delta\phi^* < 170^\circ$ in each x_{Bj} bin. Data are compared to NLO 3-jet (full line) and NLO 2-jet (dashed line) calculations obtained using the NLOJET++ program. The error band represent the scale uncertainty as described in the text.*

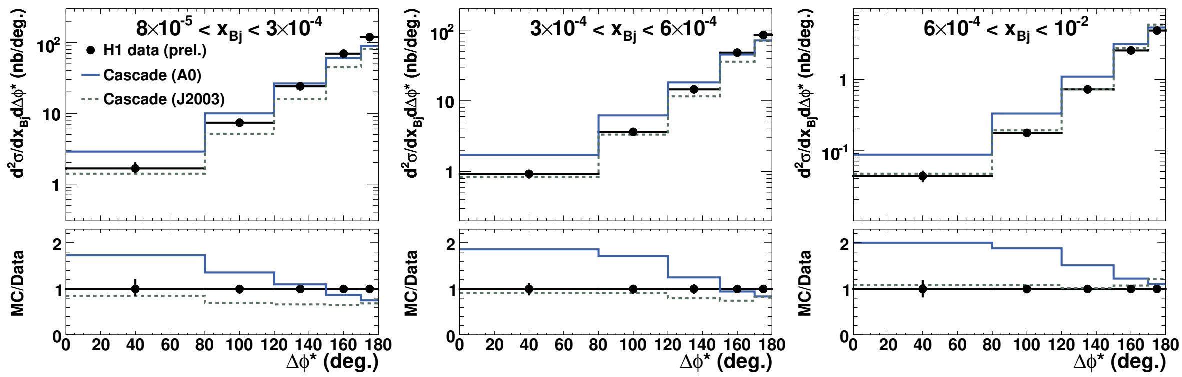

Figure 3: *Dijet cross sections as a function of $\Delta\phi^*$ in bins of x_{Bj} compared to the predictions of CASCADE using two different uPDFs.*

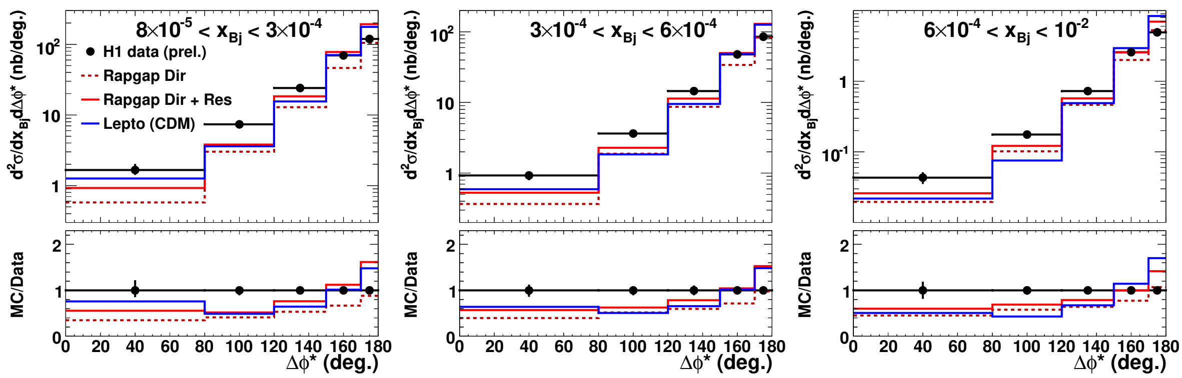

Figure 4: *Dijet cross sections as a function of $\Delta\phi^*$ in bins of x_{Bj}. Data are compared to RAPGAP DIR (red dashed line), RAPGAP DIR+RES (red full line) LEPTO(CDM) (blue full line).*

In Figure 4, data is compared to the predictions of RAPGAP DIR, RAPGAP DIR+RES and LEPTO(CDM). RAPGAP DIR predicts about the right amount of back-to-back jets but produces too few dijets with small $\Delta\phi^*$. The situation at small $\Delta\phi^*$ is somewhat improved by adding the resolved photon component, but this on the other hand also adds too many back-to-back jets. Also LEPTO(CDM) predicts too many back-to-back jets, but in contrast to RAPGAP DIR+RES, LEPTO(CDM) is closer to data at low x_{Bj} than at high x_{Bj}.

In addition to the dijet cross sections in bins of x_{Bj}, the same observable has also been measured in bins of Q^2, shown in Figures 5 - 7. In Figure 5 we again see that one parton radiation (NLO 2-jet) fails to describe the data, whereas two parton radiation (NLO 3-jet) improves the situation but is still systematically low for $\Delta\phi^* < 150°$. Data is, however, described within the large scale uncertainties. Figure 6 shows the same data compared to CASCADE. Using the uPDF J2003, CASCADE is able to describe the data except in the lowest and highest Q^2 bins, while CASCADE(A0) fails in all bins. Comparisons to RAPGAP DIR, RAPGAP DIR+RES and LEPTO(CDM) is shown in Figure 7. Again, all models fail to describe the shape of the data, predicting too few dijets with small azimuthal separations and, in the case of RAPGAP DIR+RES and LEPTO(CDM), too many back-to-back jets.

6 Summary

Dijet cross sections are presented as a function of the separation in azimuthal angle $\Delta\phi^*$ between the two jets, in bins of x_{Bj} and Q^2. One parton radiation in addition to the dijet system (NLO 2-jet) is not sufficient to describe the data. Two parton radiation (NLO 3-jet) improves the situation but is systematically low. However, data is described within the large scale uncertainties. Normalising the cross sections to the visible cross section, the scale uncertainties of the NLO calculations partially cancel, such that both NLO calculations are unable to describe the data. A sensitivity to the unintegrated gluon density is observed. Hence, the data can be used to gain further information about the k_t-dependence of the unintegrated gluon densities. RAPGAP DIR, RAPGAP DIR+RES and LEPTO(CDM) fail to describe the data in all bins.

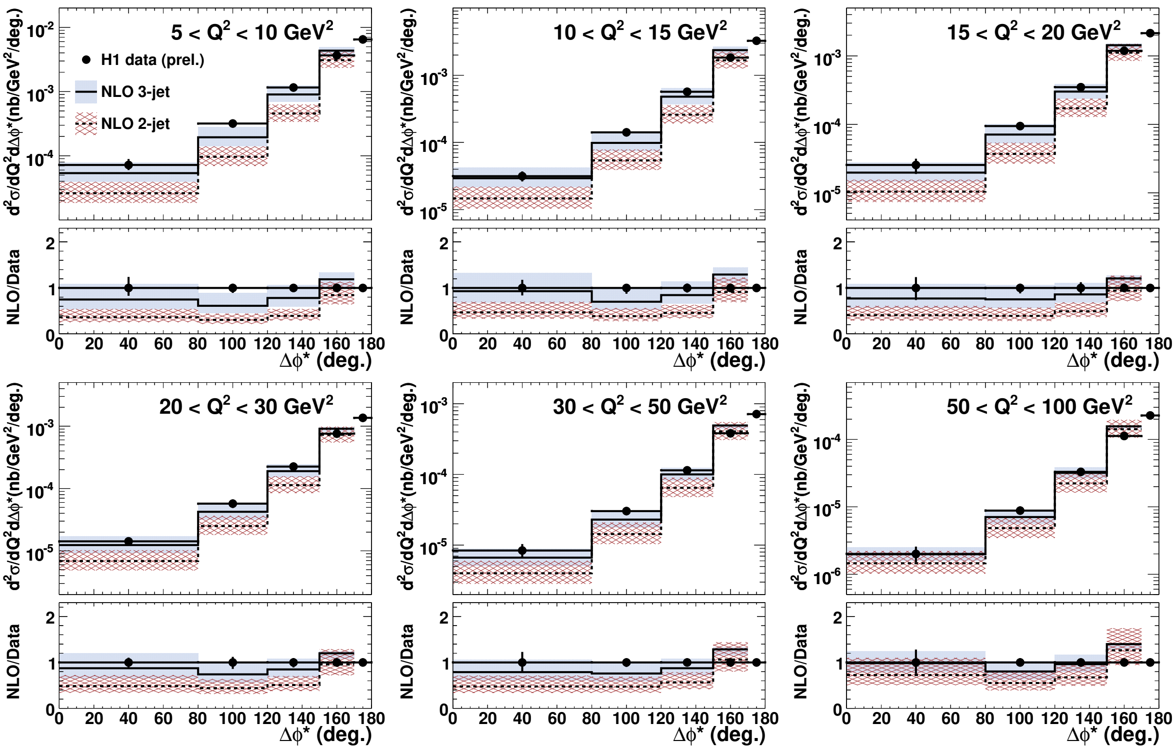

Figure 5: *Dijet cross sections as a function of $\Delta\phi^*$ in bins of Q^2. Data are compared to NLO 3-jet (full line) and NLO 2-jet (dashed line) calculations obtained using the NLOJET++ program. The error band represent the scale uncertainty as described in the text.*

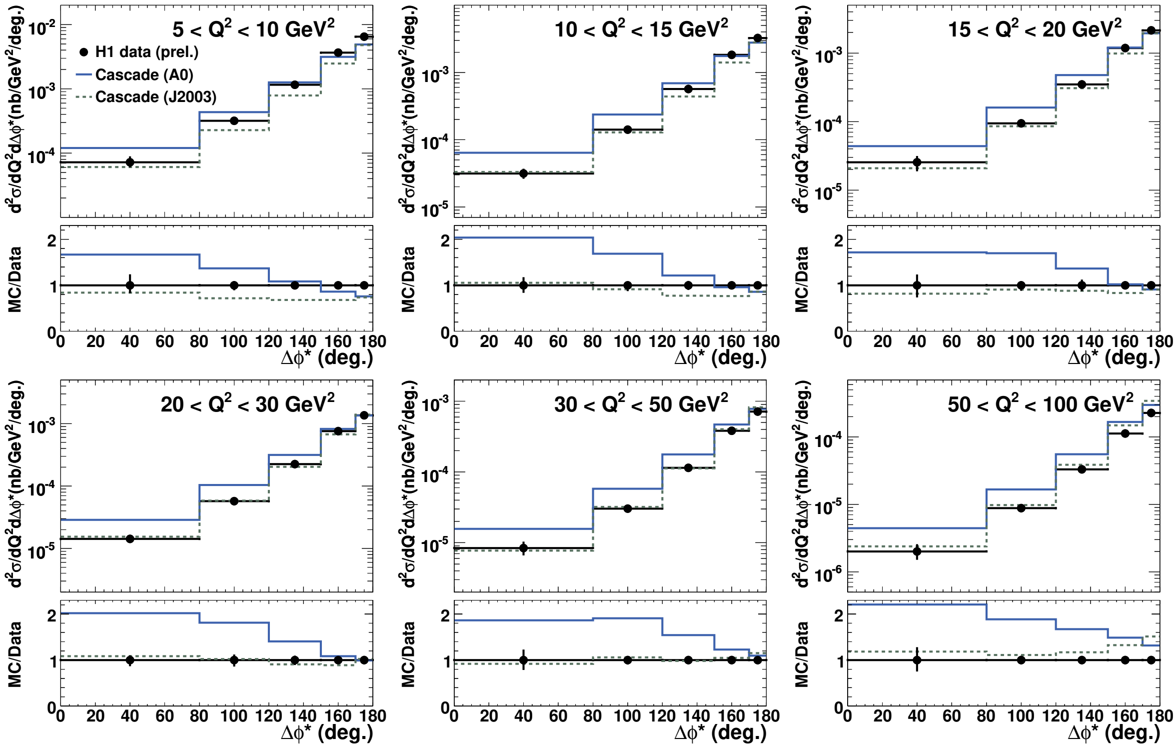

Figure 6: *Dijet cross sections as a function of $\Delta\phi^*$ in bins of Q^2 compared to the predictions of CASCADE using two different uPDFs.*

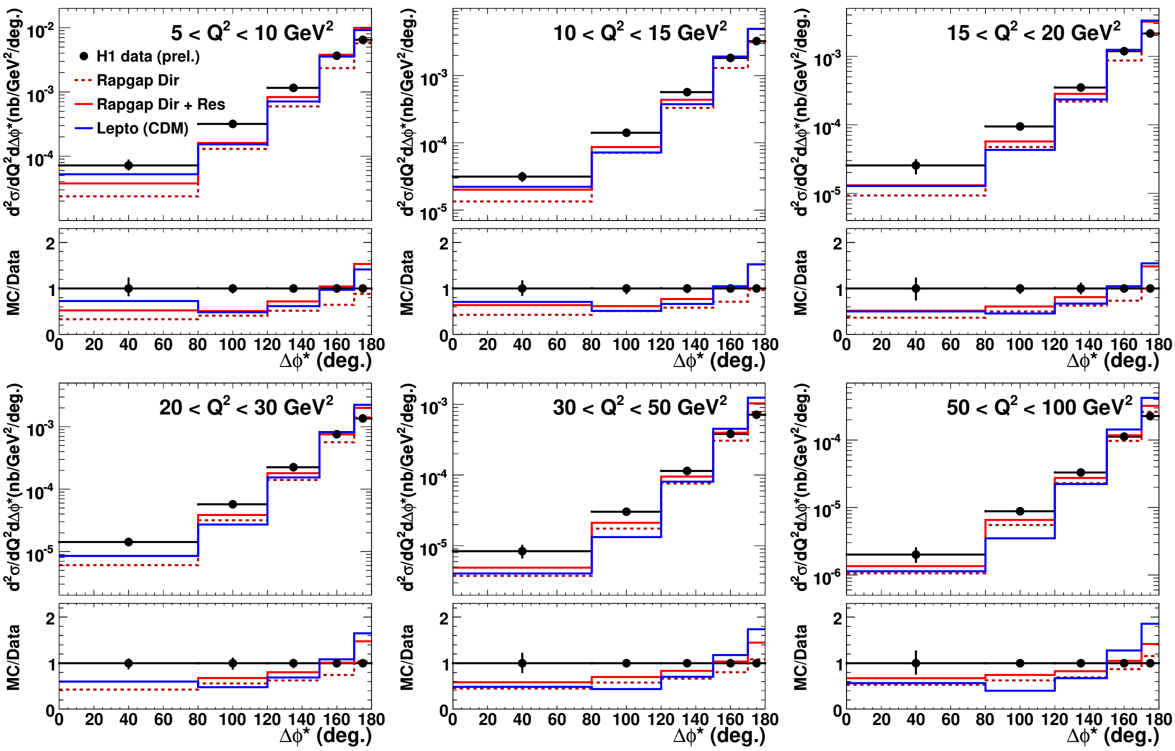

Figure 7: *Dijet cross sections as a function of* $\Delta\phi^*$ *in bins of* Q^2. *Data are compared to RAPGAP DIR (red dashed line), RAPGAP DIR+RES (red full line) LEPTO(CDM) (blue full line).*

References

[1] V. N. Gribov and L. N. Lipatov, Sov. J. Nucl. Phys. **15** (1972) 438

V. N. Gribov and L. N. Lipatov, Sov. J. Nucl. Phys. **15** (1972) 675

L. N. Lipatov, Sov. J. Nucl. Phys. **20** (1975) 94

G. Altarelli and G. Parisi, Nucl. Phys. B **126** (1977) 298.

Y. L. Dokshitzer, Sov. Phys. JETP **46** (1977) 641

[2] A. J. Askew, D. Graudenz, J. Kwiecinski and A. D. Martin, Phys. Lett. B **338** (1994) 92 [arXiv:hep-ph/9407337].

[3] E. A. Kuraev, L. N. Lipatov and V. S. Fadin, Sov. Phys. JETP **44** (1976) 443

E. A. Kuraev, L. N. Lipatov and V. S. Fadin, Sov. Phys. JETP **45** (1977) 199

I. I. Balitsky and L. N. Lipatov, Sov. J. Nucl. Phys. **28** (1978) 822

[4] M. Ciafaloni, Nucl. Phys. B **296** (1988) 49.

S. Catani, F. Fiorani and G. Marchesini, Phys. Lett. B **234** (1990) 339.

S. Catani, F. Fiorani and G. Marchesini, Nucl. Phys. B **336** (1990) 18.

G. Marchesini, Nucl. Phys. B **445** (1995) 49 [arXiv:hep-ph/9412327].

[5] I. Abt *et al.* [H1 Collaboration], Nucl. Instrum. Meth. A **386** (1997) 310.

[6] I. Abt *et al.* [H1 Collaboration], Nucl. Instrum. Meth. A **386** (1997) 348.

[7] S. Bentvelsen, J. Engelen and P. Kooijman, Reconstruction of (x,Q^2) and Extraction of Structure Functions in Neutral Current Scattering at HERA, in *Proc. of the Workshop on Physics at HERA. Vol. 1*, edited by W. Buchmüller and G. Ingelman, page 23, Hamburg, 1991, DESY, NIKHEF-H-92-02.

[8] S. D. Ellis and D. E. Soper, Phys. Rev. D **48** (1993) 3160 [arXiv:hep-ph/9305266].

[9] M. Peez, B. Portheault and E. Sauvan, *An Energy Flow Algorithm for Hadronic Reconstruction In OO: Hadroo2*, H1 internal note (2005). H1-IN-616.

[10] R. Engel, Z. Phys. C **66** (1995) 203.

[11] H. Jung, Comput. Phys. Commun. **86** (1995) 147.

[12] A. Kwiatkowski, H. Spiesberger and H. J. Mohring, Comput. Phys. Commun. **69** (1992) 155.

[13] J. Pumplin, D. R. Stump, J. Huston, H. L. Lai, P. Nadolsky and W. K. Tung, JHEP **0207** (2002) 012 [arXiv:hep-ph/0201195].

[14] G. A. Schuler and T. Sjostrand, Phys. Lett. B **376** (1996) 193 [arXiv:hep-ph/9601282].

[15] H. Jung and G. P. Salam, Eur. Phys. J. C **19** (2001) 351 [arXiv:hep-ph/0012143].

[16] H. Jung, arXiv:hep-ph/0411287.

[17] M. Hansson and H. Jung, arXiv:hep-ph/0309009.

[18] K. Charchula, G. A. Schuler and H. Spiesberger, Comput. Phys. Commun. **81** (1994) 381.

[19] G. Ingelman, A. Edin and J. Rathsman, Comput. Phys. Commun. **101** (1997) 108 [arXiv:hep-ph/9605286].

[20] L. Lonnblad, Comput. Phys. Commun. **71** (1992) 15.

[21] B. Andersson, G. Gustafson, G. Ingelman and T. Sjostrand, Phys. Rept. **97** (1983) 31.

[22] T. Sjostrand, Comput. Phys. Commun. **39** (1986) 347.

[23] Z. Nagy and Z. Trocsanyi, Phys. Rev. Lett. **87** (2001) 082001 [arXiv:hep-ph/0104315].

[24] M. A. Kimber, A. D. Martin and M. G. Ryskin, Phys. Rev. D **63** (2001) 114027 [arXiv:hep-ph/0101348].